# Summary of NIMROD (Two-Fluid) Applications

*presented by*

Carl Sovinec

*University of Wisconsin-Madison*

Pre-APS CEMM Meeting

October 28, 2012

Providence, Rhode Island

# Outline

- Drift tearing analysis and benchmarking, J. King (Tech-X Corporation)
- Update on ITG study, D. Schnack (U-WI)
- Dynamo and momentum transport, J. Sauppe and C. Sovinec (U-WI)
- Current drive and model validation for HIT-SI, C. Akcay, T. Jarboe, and C. Kim (U-WA)
- Computations for DC spheromak injection, E. Howell and C. Sovinec (U-WI)

# Drift-tearing Analysis and Benchmarking

Jacob King

*Tech-X Corporation*

Principal results:

- New drift-tearing dispersion relation
- NIMROD results agree at moderate $\beta$-values

# New dispersion relation has 2-fl Ohm's law and diamagnetic heat flows [~**b** x grad(*T*)].

- Formulation uses un-reduced extended-MHD equations.
- Electron and ion temperatures evolve separately.
- The parameter regime has large ion skin-depth and moderate $\beta$, i.e. PR4d in the Ahedo-Ramos (AR) notation.

$$\left(\hat{\gamma}+i\hat{\omega}_{*e}\right)\frac{\Gamma\left[\left(3+\bar{\tau}_Q/\bar{\sigma}\right)/4\right]}{\Gamma\left[\left(1+\bar{\tau}_Q/\bar{\sigma}\right)/4\right]}=S_g^{-1/2}\sqrt{\hat{k}_{\|}'\hat{d}_i}\,\frac{\hat{\Delta}'}{2\pi}$$

- Normalizations are with respect to $\tau_A$ and $k_{\mathrm{perp}}$.
- $\tau_Q$ is a generalization of $\tau$ from AR to include diamagnetic heat flux, grad-$p_e$, and electron-advection effects.
  - It is most significant at small $\beta$-values.

# Computations use parameters of previous comparison with AH, incorporating spatially varying $p_0$.

**Moderate $\beta$-value (0.1) makes $\tau_Q/\sigma$ small, and in this drift regime (PR3d), single-$T$ computations and analytics agree.**

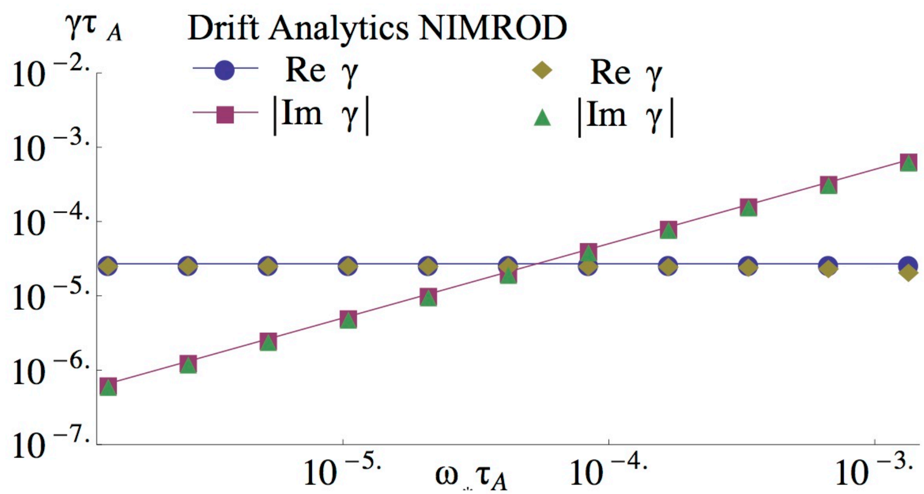


**This comparison at small $\beta$-value (0.0016) also has single-$T$ modeling with grad-$p_e$ effects in Ohm's law.**

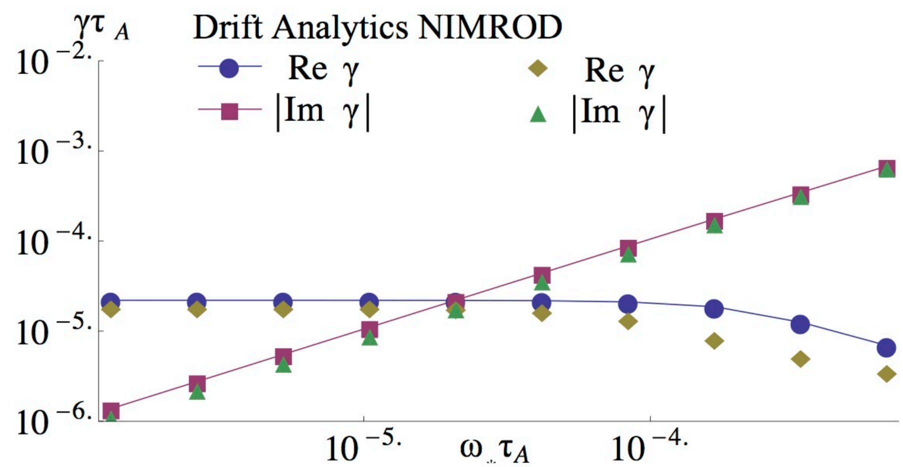


**Increasing grad-$p_0$ ➔ .   Δ' is ~constant.**

The new analytical prediction for low-$\beta$ appears similar to the single-*T* result, and two-*T* modeling requires the diamagnetic heat flows.

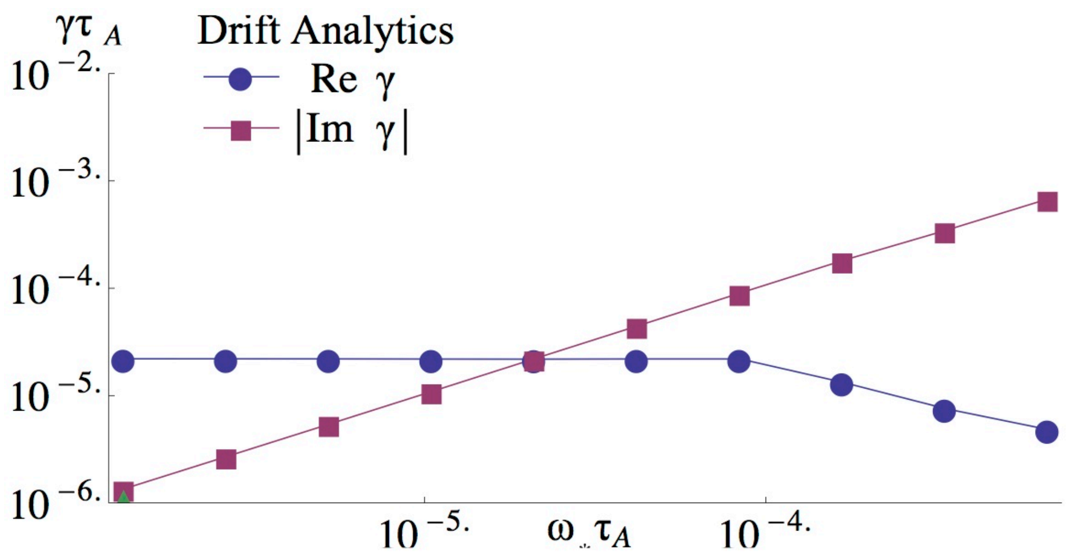


**Increasing grad-$p_0$ ➔ . Δ' is constant.**

- Two-temperature analytics predicts that the stabilizing effect at large grad-$p_0$ is absent without diamagnetic heat flow.
- NIMROD two-*T* computations in this regime have proven to be challenging (so far).

# Update on ITG Study


Dalton Schnack

*University of Wisconsin-Madison*

*in collaboration with*

Dan Barnes, Jianhua Cheng, Chris Hegna, Eric Held, Jake King, Scott Kruger, Scott Parker, Carl Sovinec, and Ping Zhu

# Ion Temperature Gradient (ITG) Instability

- ITG requires 2-fluid/FLR effects for instability
  - *g*-mode is stabilized by 2-fluid/FLR
  - Good validation test for 2-fluid/FLR computations
- Parallel ion sound wave driven unstable in presence of ion temperature gradient
  - $\eta_i = d \ln T_{i0} / dx > \eta_i^{crit}$
  - Interaction between parallel sound wave and perpendicular drift wave
  - Model problem in slab geometry
- Direct comparison of linear growth rate and real frequency in fluid regime ($k_{\mathrm{perp}} \rho_i$ <~ 0.25):
  - Local fluid theory (dipersion relation)
  - Local kinetic theory (dispersion relation)
  - Global NIMROD linear computations
- Comparison between global fluid and kinetic models underway

Computations presented here have their largest *n* and *T* gradients near center of domain.

- Profiles are hyperbolic tangents to avoid boundary effects.
- Location of largest local-theory growth-rate occurs at *x*-values just below *x*=0.

# ITG Growth Rate and Real Frequency

Growth Rate vs. $k_{perp}\, \rho_i$

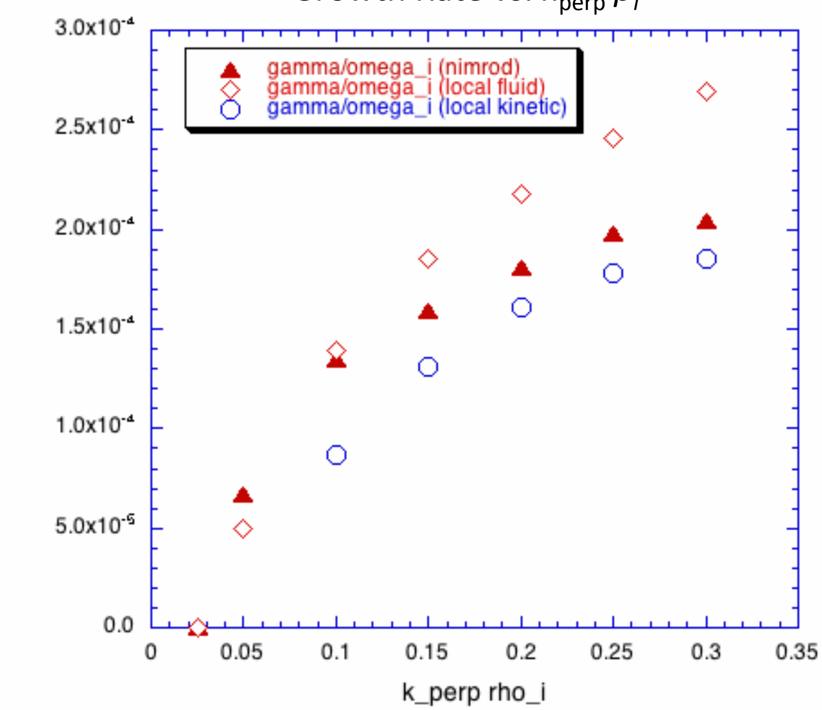


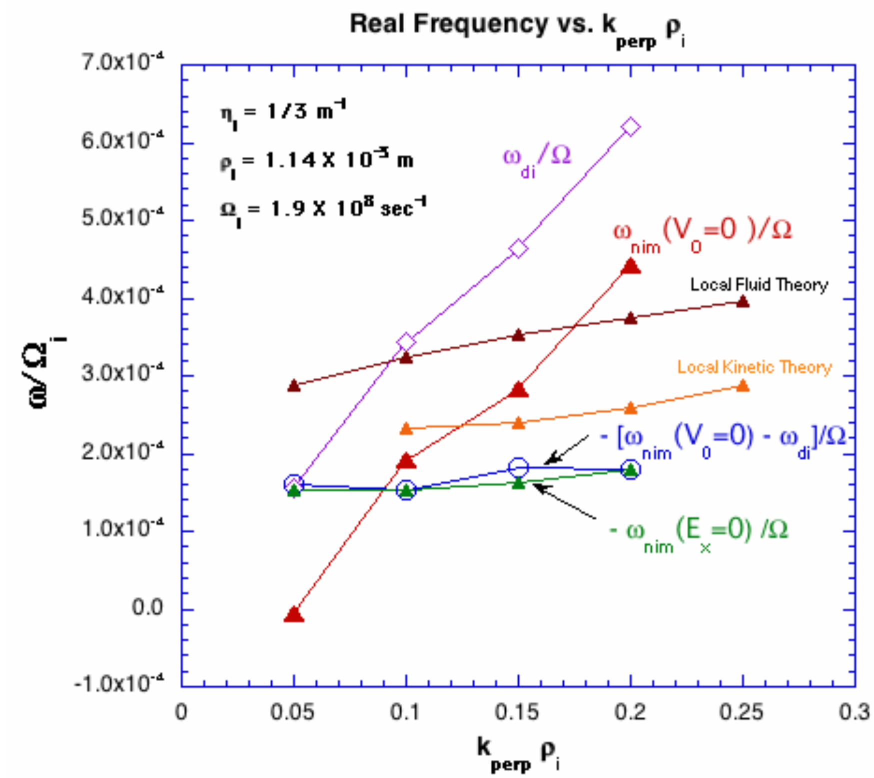


Normalized to ion cyclotron frequency

$\eta_i$ = 1/3 $m^{-1}$

$\rho_i$ = 1.14 X $10^{-3}$ m

$\Omega_i$ = 1.9 X $10^{8}$ $sec^{-1}$

- $\omega_{di}$   Ion Diamagnetic Frequency
- $\omega_{nim}(V_0 = 0)$   No Eq. Velocity (Doppler shift)
- $\omega_{nim}(E_x = 0)$   No Eq. Elec. Field (No Doppler shift)
- Minus sign (-) means mode propagates *opposite* the ion drift

# Summary/Caveats

- Direct comparison between:
  - Local fluid theory
  - Local kinetic theory
  - Global NIMROD linear computations
- Reasonably good agreement
  - Validation of NIMROD 2-fluid/FLR model (Braginskii) and algorithm?
- Caveats: computational signal-analysis diagnostic finds $\gamma$ and $\omega_r$ to be weak functions of $x$
  - Presence of other mode activity?
  - Numerical instability with $k_y$ dependence appears at late times
- Major questions:
  - Why is the real frequency negative?
    - Disagrees with local theory (fluid and kinetic)
  - Why are $\gamma$ and $\omega_r$ functions of $x$?
    - Impossible for a global eigenvalue
  - Why does the eigenfunction depend on the frame of reference ($E_x$)?
- Comparison with GK computation (CU group) will use a smaller domain.

# Dynamo and Momentum Transport

Josh Sauppe and Carl Sovinec
*Univ. of Wisconsin-Madison*

Principal results:

- Background flow breaks the symmetry of relaxation
- Background flow affects both Hall and MHD dynamos

# Background flow breaks the symmetry of relaxation relative to positive and negative current.

- Results with negative current, $\mathbf{J}_0 \cdot \mathbf{B}_0 < 0$, exhibit approximately twice as much field-reversal during the first relaxation event.
- Somewhat more nonlinear coupling occurs, as evident from the larger spectral width, $N_s \equiv \left(\sum_n W_{1,n}\right)^2 \Big/ \sum_n W_{1,n}^2$, where $W_{1,n}$ is the magnetic fluctuation energy in the (m=1,n) component.

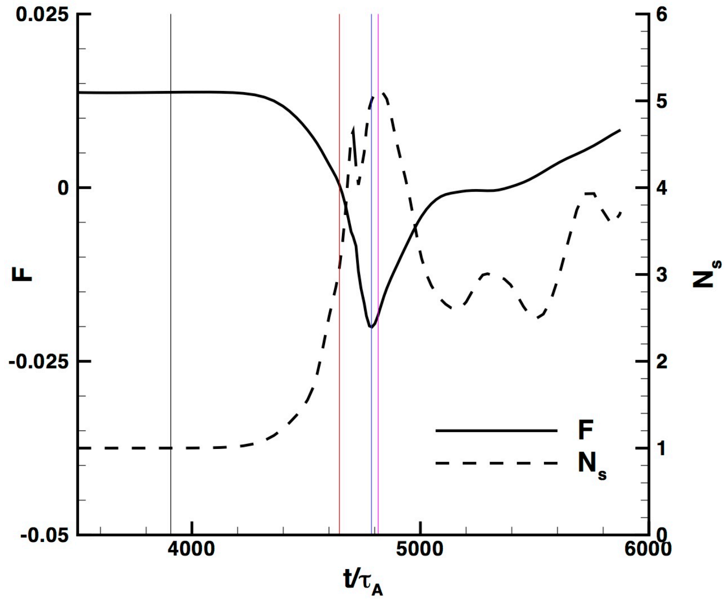


**Evolution of reversal parameter (*F*) and spectral width ($N_s$) for positive current.**

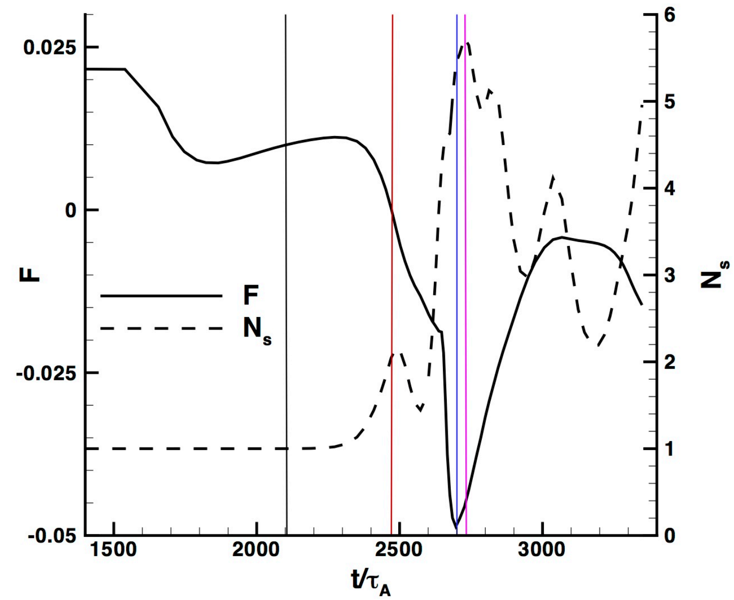


**Evolution of *F* and $N_s$ with negative current.**

# Background flow alters Hall and MHD dynamo effects.

- At reversal the sum is similar for the two current orientations, but the contributions oppose each other with positive current.

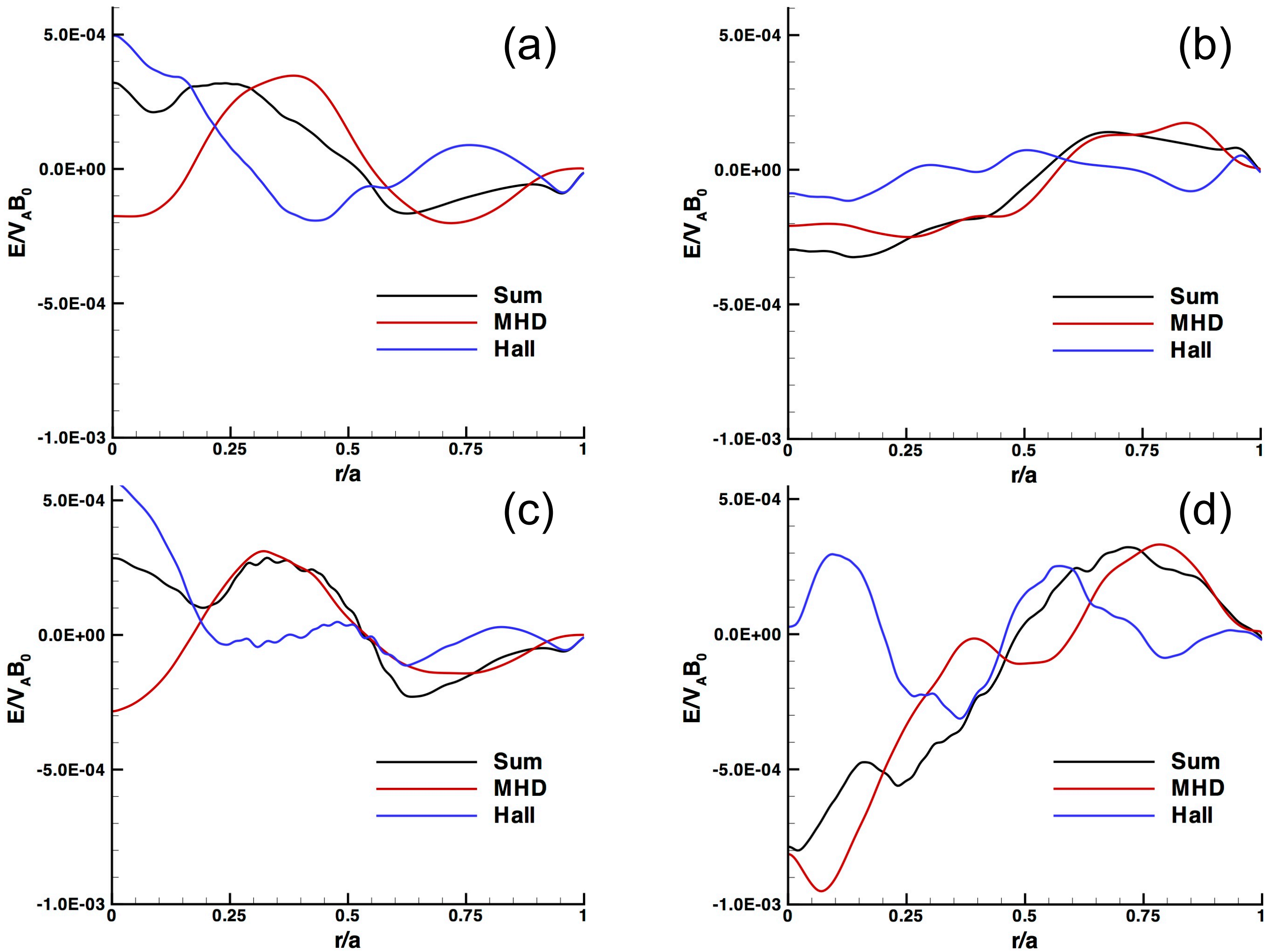


**Dynamo contributions at initial reversal with (a) $J_0 \bullet B_0 > 0$ and (b) $J_0 \bullet B_0 < 0$ and at greatest reversal with (c) $J_0 \bullet B_0 > 0$ and (d) $J_0 \bullet B_0 < 0$.**

# Current Drive and Model Validation for HIT-SI

Cihan Akcay, Charlson Kim, and Tom Jarboe

*Univ. of Washington / Plasma Science and Innovation Center*

Principal results:

- Two-fluid computations reproduce current rectification/multiplication
- Synthetic diagnostics show very substantial agreement with laboratory measurements.

# SIHI is implemented as a set of normal magnetic field $B_n$ and tangential electric field $\mathbf{E}_t$ boundary conditions imposed at the annular boundaries

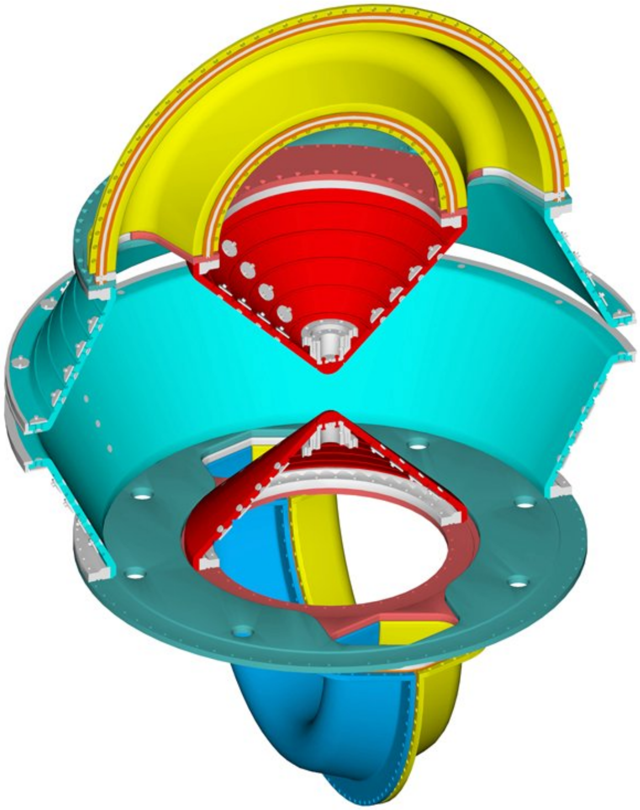

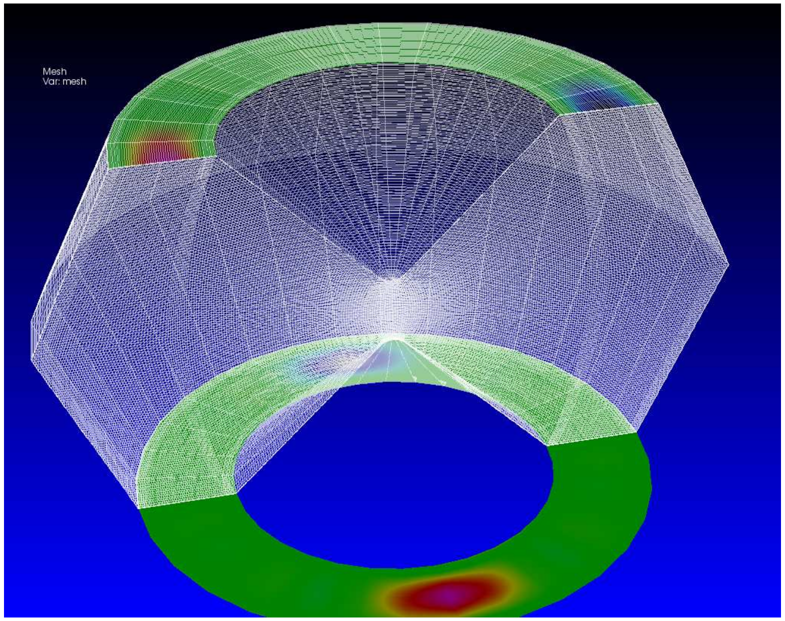


A MATLAB GS solver is used to obtain the functional form for $B_n$ and $E_t$, which are hard-coded in NIMROD in `B_norm` and `E_tang`.

# Highlight

- Two-fluid MHD (2fl MHD)
  - shows greater current amplification $\frac{I_{tor}}{I_{inj}}$ and faster current rise times than rMHD.
  - reproduces $\frac{I_{tor}}{I_{inj}}$ demonstrated by HIT-SI at $f_{inj} = 14.5$ kHz.
  - shows good agreement with the experimental data: **validation**.
  - figure compares time-averaged magnetic profiles.

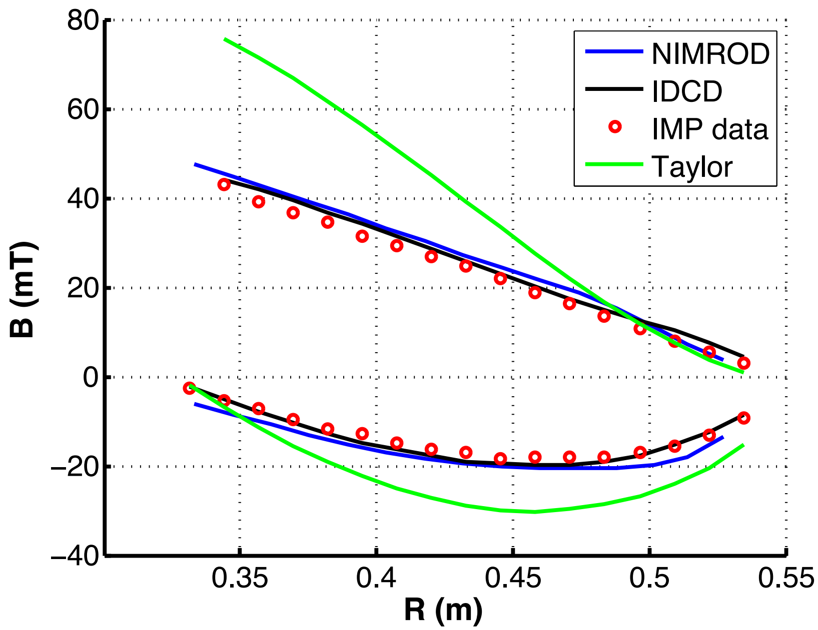

# Comparison of IMP time traces at various radial locations with NIMROD synthetic probes.

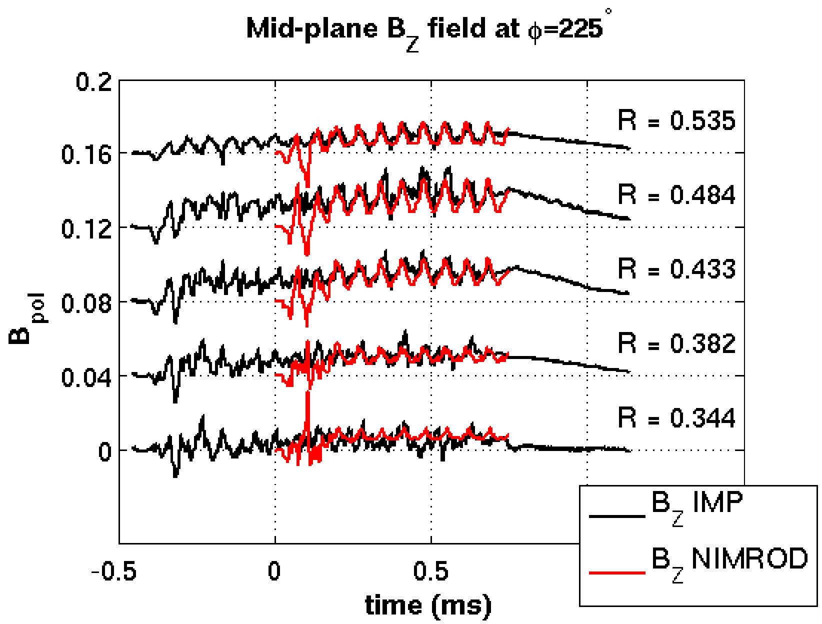


(s) 6 eV 2fl MHD with $\frac{I_{tor}}{I_{inj}} = 1.7$

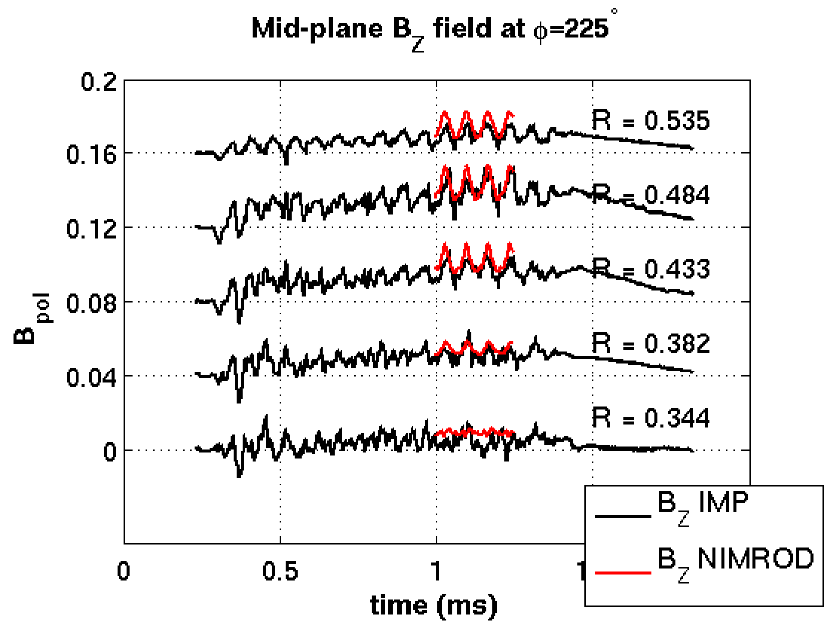


(t) 13eV 2fl MHD with $\frac{I_{tor}}{I_{inj}} = 3$

# Computations for DC Injected Simulations

Eric Howell and Carl Sovinec
*Univ. of Wisconsin-Madison*

Principal nonlinear result:

- Two-fluid computation from partially saturated MHD computation continues flux amplification without DC power.

# 2-fluid effects improve the performance for the partial formation case early into the decay.

- The poloidal flux amplification that occurs early into the decay results in 6% more flux.
- A rise in peak temperature is observed earlier in time.
- No difference is observed between the MHD and 2-fluid simulations early in the decay phase for the fully saturated case.

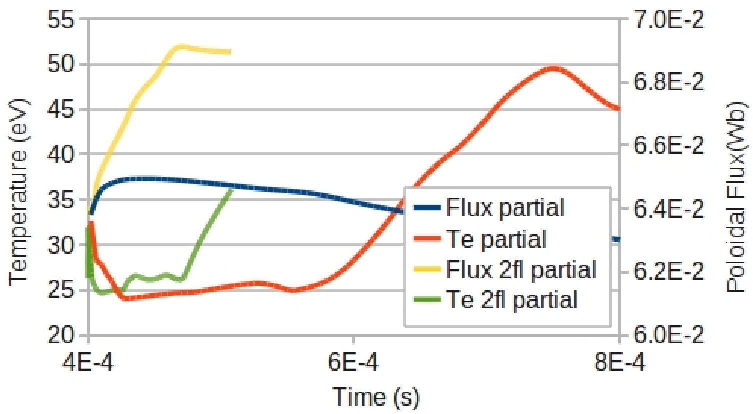

# NIMROD-related presentations, APS 2012

1. BP8.00069, NIMROD Modeling of the Compact Toroidal Hybrid (CTH), Hebert
2. CP8.00014, Dynamos in spherical time-periodic flows, Khalzov
3. CP8.00045, Quasilinear dynamo effects in two-fluid RFP Model, Mirnov
4. GP8.00124, Edge plasma response to resonant magnetic perturbation in extended MHD model, Zhu
5. JP8.00105, Simulations of validation platform experiments by the PSI-Center, Nelson
6. JP8.00106, NIMROD sims. of the stabilization of the FRC tilt instability with energetic ion beams, Milroy
7. JP8.00107, Implementing a reacting plasma-neutral model in the NIMROD finite element code, Norgaard
8. JP8.00109, Implementation of higher-order moment equations in NIMROD, Ji
9. JP8.00124, Eigenmode tests of improved basis functions for NIMROD, Sovinec
10. JP8.00147, Two-fluid modeling of current and flow relaxation in the reversed-field pinch, Sauppe
11. NI3.00003, Self-consistent simulations of nonlinear MHD and profile evolution in stellarator configurations, Schlutt*
12. NP8.00069, Simulations of current-filament dynamics and relaxation in the Pegasus ST, O'Bryan
13. NP8.00095, Generalized resistive wall boundary conditions for cylindrical and toroidal geometry in NIMROD, Montgomery
14. NP8.00096, Extended-MHD studies of flow-profile effects on edge harmonic oscillations in QH-mode discharges, King
15. NP8.00107, On the stability of a particle driven Alfven mode localized within the minimum q in reversed shear, Brennan
16. PI2.00003, Impurity mixing, radiation asymmetry, and runaway electron confinement in MGI simulation of DIII-D and ITER, Izzo*
17. PP8.00025, Flux-surface closure during resistive-MHD simulations of coaxial helicity injection (CHI) in NSTX, Hooper
18. PP8.00048, FRC edge physics using NIMROD, Necas
19. PP8.00052, Analysis and measurement of the 3D magnetic field in a rotating magnetic field driven FRC, Velas
20. PP8.00056, Overview of HIT-SI progress and results, Victor
21. PP8.00057, Measurements of ion temperature and velocity in HIT-SI with comparison to NIMROD calculations, development of piezoelectric valve, Hossack
22. PP8.00059, Extended MHD NIMROD simulations of HIT-SI plasmas, Akcay
23. PP8.00063, Extended MHD simulations of spheromaks, Howell
24. TP8.00055, ECCD-induced tearing mode stabilization via active control in coupled NIMROD/GENRAY HPC simulations, Jenkins
25. UP8.00057, Roll-back planning for a compact fusion system, Woodruff

*INVITED TALK